Manuscript submitted to AIMS Journal

doi:10.3934/xx.xxxxxxx

A VECTOR ALLEE EFFECT IN MOSQUITO DYNAMICS

J. Banasiak[✉*1], Bime M. Ghakanyuy [✉1,2] and Gideon A. Ngwa [✉3]

[1]Department of Mathematics and Applied Mathematics, University of Pretoria, South Africa

[2]Department of Mathematics and Computer Science, University of Bamenda, Cameroon

[3]Applied Mathematical and Computer Assisted Modelling Unit, Department of Mathematics, University of Buea, Cameroon

(Communicated by Handling Editor)

Abstract. We consider a recently introduced model of mosquito dynamics that includes mating and progression through breeding, questing and egg-laying stages of mosquitoes using human and other vertebrate sources for blood meals. By exploiting a multiscale character of the model and recent results on their uniform-in-time asymptotics, we derive a simplified monotone model with the same long-term dynamics. Using the theory of monotone dynamical systems, we show that for a range of parameters, the latter displays Allee-type dynamics; that is, it has one extinction and two positive equilibria ordered with respect to the positive cone $\mathbb{R}^7_+$, with the extinction and the larger equilibrium being attractive and the middle one unstable. Using asymptotic analysis, we show that the original system also displays this pattern.

1. **Introduction.** Understanding the life cycle of mosquitoes is of utmost importance in any attempt to control diseases caused by them, such as malaria, dengue, zika or chikungunya, see, e.g., [15, 18, 31]. The problem is that it is pretty complex. Broadly, the cycle can be divided into the aquatic and terrestrial stages. In the aquatic stage, we have eggs, several larval stages and pupae, which hatch into terrestrial juvenile male and female mosquitoes who mate, and the female fertilized (breeding) mosquitoes quest for blood necessary for the development of eggs. The fed female mosquitoes lay eggs and return to the breeding stage.

There is abundant literature on modelling the mosquito life cycle, so the survey below is restricted to papers we consider to be relevant to our study. Depending on the needs, models have different levels of resolution, focusing on particular parts of the cycle and simplifying or discarding the others. For instance, in the series of papers [26, 27, 28], the authors develop a model with aquatic and terrestrial stages which is then joined to a malaria model or combined with a sterile insect population. In these models, the authors do not consider sex differences, while mating is implicitly included in the form of mating rate. In contrast, [2] deals with male and female mosquitoes and the aquatic stage but disregards the mating and questing processes. Sex-structured mosquito populations were considered in [1, 40,

2020 *Mathematics Subject Classification.* Primary: 34E13, 34E15, 34D23, 92D30, 92-10.

Key words and phrases. Multiscale malaria models, singularly perturbed problems, uniform in time asymptotics, global stability of solutions.

The authors were supported by the DSI/NRF SARChI M3B2 grant N 82770.

GAN acknowledges the Cameroonian Ministry of Higher Education through the initiative for the modernization of research in Cameroons Higher Education.

*Corresponding author: J. Banasiak.

47]. The first one deals with a general insect population, where males and females emerge from an "immature" stage and mate according to a complex mechanism. In the second one, the authors deal with mosquitoes and consider the aquatic stage and mating where, assuming that the males are spread according to the Poisson distribution, see, e.g., [16, Eq. (1)], the mating occurs with the same probability if there is at least one male in a prescribed vicinity of the female. In the last one, the authors split the logistic model for the total mosquito population by assuming that the ratio between male and female offspring produced by a female is constant.

On the other hand, in modelling mosquito-borne diseases, it is essential to recognize that a female mosquito must bite two times, an infected and then a susceptible human, to transmit the disease. Thus, paying closer attention to the gonotrophic cycle between the breeding and ovipositing stages becomes important; see [30], but we shall not pursue this direction here.

Our interest lies in the occurrence of the so-called Allee effect in the model introduced in [31]. The Allee effect, that is, the situation in which populations with size smaller than a certain threshold die out, is quite common in nature and, in particular, in insect populations, [16]. The existence of such a threshold proved to be important in pest management by the sterile insect technique consisting in introducing sterile individuals into a wild population to change the natural Allee threshold so that the population finds itself below it and dies out. Several previously mentioned papers [27, 28, 40, 47] are concerned with the design of a sterile insect control of mosquitoes and thus of particular interest is the occurrence of an Allee effect in the population. To achieve this in the wild population, the authors propose various ways to induce the desired effect in the system. For instance, in [28, Section 2.2], the adult birth rate (equivalent to the oviposition rate in our model) is appropriately modified, while in [47, Section 2.2], the authors modify the mating mechanism by introducing an appropriate mating rate. Similarly, in [40], the authors use the Poisson distribution, proposed in [16] as one way of relating the probability of a female mating to the density of males, but they do not consider separately the wild population. It is also worthwhile to mention the recent paper [22] discussing discrete versions of the above results.

In this paper, we present an alternative way of deriving models of mosquito populations displaying an Allee effect. Our model is based on the ideas of [42, Chapter 7] and uses multi-scale analysis of a larger meta-system with much simpler mating dynamics given by the mass-action law. While we recognize many shortcomings of the mass-action law, it is still a widely used tool to model animal interactions, see, e.g., [39] and the references therein. In our opinion, it is interesting to show that complex models, developed from the first principles in the papers mentioned above, can be derived by quasi-steady state approximation from such simple dynamics, confirming thus the observation in [46] that "the power-law format is amazingly rich and that it indeed constitutes a canonical format that permits the design and analysis of models in a rigorously prescribed manner." More precisely, we will consider the model introduced in [31], whose flowchart is presented in Fig. 1. The complexity of the model and lack of a clear structure makes its comprehensive analysis difficult, so [31] contains only a preliminary description of its dynamics. On the other hand, the model is driven by several processes with different rates. For instance, mating occurs quickly after the emergence of female mosquitoes to ensure the passage of their genes to the next generation, [44]. Consequently, the dynamics of juvenile mosquitoes can be considered to be much faster than that of aquatic

State Variables	Description of Variables
A	Density of aquatic life forms
F_B	Density of newly emerged (unfertilized) female mosquitoes
M_B	Density of newly emerged male mosquitoes
B	Density of fertilized female mosquitoes
Q_H	Density of fertilized female mosquitoes questing human blood
Q_V	Density of fertilized female mosquitoes seeking non human blood
R_V	Density of mosquitoes that successfully fed from nonhuman source
R_H	Density of mosquitoes that successfully fed from humans
H	Constant human population density
V	Constant vertebrate population density

TABLE 1. Description of state variables

and adult forms. Also, there is evidence, [13, 19, 44], that the life span of newly hatched male mosquitoes is much shorter than that of the females. These factors motivate the possibility of considering the system as a multiscale one and exploiting this property to simplify by using the quasi-steady state (QSS) approximation, which can be justified, at least for big rates difference, by the methods of the singular perturbation theory, [7, 21, 25], as done in [8, 9, 32, 33, 34]. Moreover, by more refined techniques of [4, 23], it is possible to show that the simplified models have the same long-term dynamics as the original one. We acknowledge that while not always realistic empirical data make the QSS approximation plausible from the mathematical point of view, the numerical simulations show its validity. Hence, QSS approximation approach can serve as a useful guideline for reducing the complexity of the model.

The paper has the following structure. In Section 2, we introduce the model and discuss its multiscale versions and resulting simplified, cooperative systems, allowing for a reasonably complete description of their long-term dynamics. We focus on the case with a large death rate of the juvenile males and provide a detailed description of its dynamics in Section 3. In particular, we show the existence of a saddle-node bifurcation of equilibria. An interesting feature here is that the bifurcation leads to the creation of three equilibria, the trivial and two positive ones, which, moreover, are ordered (with respect to the positive orthant of the state space). Furthermore, the trivial and the largest equilibria are globally asymptotically stable in adjoining order intervals. In contrast, the middle equilibrium is unstable, which shows that the model exhibits a vector Allee effect. In Section 4, we apply the results of [3, 4] to discuss the relevance of the analysis of the simplified model to the long-term dynamics of the original one and in Section 5, we present simulations showing, in particular, that the former provides a good approximation to the latter even for relatively small differences between the juvenile male and female mosquitoes death rates. Finally, Section 6 contains conclusions.

2. The model and its asymptotic reduction.

To describe the model, we introduce the state variables in Table 1 and their interactions in the flow chart in Figure 1. The total mosquito population is divided into two broad groups: the

aquatic forms denoted by the symbol A and the terrestrial forms denoted by one of the symbols $F_B, M_B, B, Q_h, Q_V, R_H, R_V$ whose description is given in Table 1. The aquatic stage, A, is a class comprising the eggs, larvae, and pupae, which are interpreted as aquatic biomass from which terrestrial forms emerge. The terrestrial forms are further divided into compartments, where we base the compartmentalization on the fact that the mosquito undergoes a reproductive cycle called the gonotrophic cycle so that at each time each adult female mosquito's physiological state (well fed with a sugar meal, well nourished with a blood meal, rested after blood feeding, oviposited, nulliparous, mated/fertilized, etc) on this cycle can be characterized. The male mosquitoes, F_B, are eventually counted as a fraction of the aquatic biomass, A. The adult forms of the mosquito mature from the aquatic habitat either as males, M_B, or females, F_B. Reproductive success of mosquitoes requires a newly emerged adult female mosquito to locate a mating partner followed by proper mating. For the Anopheles sp mosquito, mating occurs within the first 3-5 days of the adults life. There is a controversy over which event comes first: mating before the first blood feeding episode or taking the first blood meal before mating and whether the female mosquito re-mates at all, [45]. Here, we assume that the female *Anopheles sp* mosquito mates once and stores the spermatozoa in spermatheca after mating so that during each subsequent oviposition, the eggs can be fertilized during their transit through the oviduct [10, 11, 14, 20, 24]. We assume for this paper that mating takes place before the mosquitoes enter the blood-feeding phase so that the class B comprises female mosquitoes that are fertilized and ready to begin blood questing. Further, we assume that the encounters between male and female mosquitoes follow the mass action law. As mentioned earlier, other forms of mating models have been proposed in [40, 47], but, as we shall see below, they lead to the same long-term dynamics. Fully fertilized females become the breeding site mosquitoes. When they leave the breeding site, they can either quest for blood meal within non-human populations, the Q_V or quest for blood meals within human populations Q_H. Mosquitoes of type Q_H interact with humans, H, with mass action contact parameter τ_H, while mosquitoes of type Q_V interact with non-humans, V, with mass action contact parameter τ_V. Mosquitoes that successfully take blood meals, with success probability p, from humans become resting mosquitoes of type R_H, while those that harvest blood meals, with success probability q, within non-human populations become resting mosquitoes of type R_V. Mosquitoes of type $R \in \{R_H, R_V\}$, after their resting period, return (at respective rates a_H and a_V per R_H and R_V) to the breeding site as type B mosquitoes to lay eggs. Eggs, laid at rate $\lambda(R)$ per reproducing mosquito of type R, enter the aquatic environment to repopulate A. Each mosquito, of type $Q \in \{Q_H, Q_V\}$, can quest for blood from human or non-human sources depending on its blood preference and the availability of the source, and it can change its preference after each oviposition. Thus, the

original model from [31] can be written as

$$\begin{aligned}
A' &= (a_H R_H + a_V R_V)\lambda(R)\left(1 - \frac{A}{L_P}\right) - (\gamma + \mu_{A1} + \mu_{A2} A)\, A,\\
M_B' &= (1-\hat{\theta})\hat{\xi}\gamma A - \hat{\mu}_{M_B} M_B,\\
F_B' &= \hat{\theta}\hat{\xi}\gamma A - S M_B F_B - \hat{\mu}_{F_B} F_B,\\
B' &= S M_B F_B + a_H R_H + a_V R_V - bB - \mu_B B,\\
Q_H' &= b\omega B - \tau_H H Q_H - \mu_{Q_H} Q_H,\\
Q_V' &= b(1-\omega) B - \tau_V V Q_V - \mu_{Q_V} Q_V,\\
R_H' &= p\tau_H H Q_H - a_H R_H - \mu_{R_H} R_H,\\
R_V' &= q\tau_V V Q_V - a_V R_V - \mu_{R_V} R_V,
\end{aligned} \tag{1}$$

where $R = R_V + R_H$. Most terms are self-explanatory with the rates described in Table 2. Transfers between stages are linear except for the oviposition, the density-

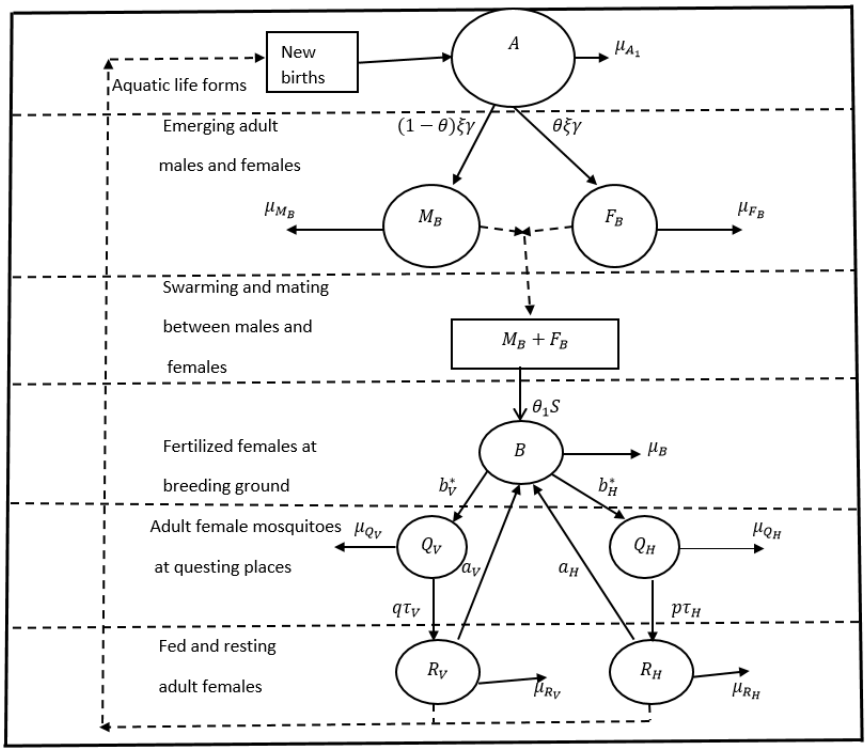

FIGURE 1. Compartments of the model.

dependent death process at the aquatic stage, see [2], and the mating, modelled using the mass action law. In the oviposition rate, given by

$$\Lambda(R_H, R_V)\left(1 - \frac{A}{L_P}\right) = (a_H R_H + a_V R_V)\lambda(R)\left(1 - \frac{A}{L_P}\right), \tag{2}$$

$\lambda(R)$ is the change in the oviposition per capita due to overcrowding. A comprehensive function description λ can be found in [31]. In general, if it is defined for

all R, it should be a non-increasing function for large R and such that $\Lambda(R_H, R_V)$ has a finite limit as $R \to \infty$. It is, however, possible that λ is only defined for some interval $[0, L]$ if a certain level of overcrowding prevents the female mosquitoes from laying eggs, [31]. Similarly, the factor $\left(1 - \frac{A}{L_P}\right)$ is specific to some mosquito species. E.g., *Aedes albopictus* (and even *Aedes aegypti*) are capable of selecting their breeding sites, seeking those with high food content and low intraspecific competition pressure. Thus, if breeding sites in a given area already contain too many larvae, the females will not deposit eggs there, see [15]. The only parameters that require explanation are γ and ξ (and $\hat{\xi}$). The need to introduce both follows because the aquatic stage is described by its biomass, while M_B and F_B are the number of individuals (or densities). Thus, γ is the rate of depletion of the aquatic biomass by the hatching of juvenile mosquitoes, and ξ is the conversion factor of the unit of aquatic biomass into individual mosquitoes. We note that in (1), we use "hatted" notation $\hat{\xi}, \hat{\mu}_{M_B}, \hat{\mu}_{F_B}$ and $\hat{\theta}$ to indicate the parameters which can be considered large (or small) in asymptotic analysis.

To complete the formulation of the above system, we complement (1) with initial conditions

$$\begin{aligned} &A(0) = \mathring{A},\ M_B(0) = \mathring{M}_B,\ F_B(0) = \mathring{F}_B,\ R_V(0) = \mathring{R}_V,\ R_H(0) = \mathring{R}_H, \\ &B(0) = \mathring{B},\ Q_V(0) = \mathring{Q}_V,\ Q_H(0) = \mathring{Q}_H, \end{aligned} \tag{3}$$

where $\mathring{A}, \dots, \mathring{Q}_H$ are all non-negative.

2.1. **Asymptotic reduction.** In this section, we formally simplify system (1) using an asymptotic approach based on the existence of multiple time scales in it. Then, the reduced systems allow for a detailed mathematical analysis, which can be translated back to the level of (1). To identify the different time scales, we refer to biological considerations.

1. There is evidence, [13, 19, 44], that the life span of newly hatched male mosquitoes M_B is much shorter than that of the females F_B, that is, $\hat{\mu}_{M_B}$ is much larger than $\hat{\mu}_{F_B}$. To ensure that despite the high mortality of the males, their population does not vanish, the recruitment rate of the males must be of a comparable magnitude. Since $\hat{\theta} \in (0, 1)$ and making γ large would drive A to extinction, the only possibility is that $\hat{\xi}$ is also large. However, if we want to keep μ_{F_B} and S at the slow-time scale, the recruitment of F_B must also be slow, which yields that $\hat{\theta}$ must be small. Thus, we re-label the parameters as $\epsilon\hat{\mu}_{M_B} = \mu_{M_B}$, $\epsilon\hat{\xi} = \xi$ and $\hat{\theta} = \epsilon\theta$, where ϵ is a small positive parameter and μ_{M_B}, ξ, θ are $O(1)$ quantities.

This argument results in the singularly perturbed system

$$\begin{aligned} A' &= \Lambda(R_H, R_V)\left(1 - \frac{A}{L_P}\right) - (\gamma + \mu_{A1} + \mu_{A2}A)\,A, \\ \epsilon M_B' &= (1 - \epsilon\theta)\xi\gamma A - \mu_{M_B} M_B, \\ F_B' &= \theta\xi\gamma A - S M_B F_B - \mu_{F_B} F_B, \\ B' &= S M_B F_B + a_H R_H + a_V R_V - bB - \mu_B B, \\ Q_H' &= b\omega B - \tau_H H Q_H - \mu_{Q_H} Q_H, \\ Q_V' &= b(1 - \omega)B - \tau_V V Q_V - \mu_{Q_V} Q_V, \\ R_H' &= p\tau_H H Q_H - a_H R_H - \mu_{R_H} R_H, \\ R_V' &= q\tau_V V Q_V - a_V R_V - \mu_{R_V} R_V. \end{aligned} \tag{4}$$

Parameter	**Description of Parameters**	**Quasi-dimension**
$\theta, \hat{\theta}$	Proportion of aquatic forms that develop into female mosquitoes.	1
γ	Rate of the aquatic forms transition into terrestrial forms.	T^{-1}
$\xi, \hat{\xi}$	Biomass transition factor from aquatic into terrestrial forms.	MA_q^{-1}
$\mu_y, \hat{\mu}_y$	Natural death rate of the mosquitoes of type y, where y denotes one of the adult mosquito-types.	T^{-1}
a_V, a_H	Return rates of reproductive females to the breeding site from to the from, respectively, vertebrates (a_V) and human (a_H) habitats.	T^{-1}
b	Rate at which mosquitoes leave the breeding site for questing.	T^{-1}
ω	The human blood preference factor.	1
τ_V	Effective mass action contact parameter between zoophilic mosquitoes and vertebrates.	$V^{-1}T^{-1}$
τ_H	Effective mass action contact parameter between anthropophilic mosquitoes and humans.	$H^{-1}T^{-1}$
p, q	Probabilities that a mosquito successfully harvests a blood meal from a human (p) or vertebrate (q) population. $0 \leq p, q \leq 1$.	1
μ_{A1}	Natural death rate per aquatic life form.	T^{-1}
μ_{A2}	Additional death due to overcrowding of aquatic forms.	$A_q^{-1}T^{-1}$
S	Constant mass action contact parameters between female and male mosquitoes.	$M^{-1}T^{-1}$
L_P	Carrying capacity of the pond.	A_q

TABLE 2. Table of parameters, their descriptions descriptions and quasi-dimensional units. The "hatted" parameters are rescaled in the process of multiscale analysis, and the "unhatted" versions are the reference values. In the quasi-dimension, A_q represents aquatic density, M mosquito density, H human density, V vertebrate density, T represents time and 1 identifies a dimensionless parameter.

Note that (4) is the same as (1) if $\epsilon = \frac{\mu_{M_B}}{\hat{\mu}_{M_B}} = \frac{\xi}{\hat{\xi}} = \frac{\hat{\theta}}{\theta}$, so ϵ is small if $\hat{\mu}_{M_B}$ and $\hat{\xi}$ are large and $\hat{\theta}$ is small. We emphasize that this does not restrict ϵ as we can choose μ_B, ξ and θ as long as they are of the same magnitude as the other parameters.

Letting $\epsilon = 0$, we arrive at the equation of the slow manifold (quasi-steady state), [7, 21, 25],

$$M_B = \frac{\xi \gamma A}{\mu_{M_B}}, \tag{5}$$

and the reduced model

$$\begin{aligned}
A' &= \Lambda(R_H, R_V)\left(1 - \frac{A}{L_P}\right) - (\gamma + \mu_{A1} + \mu_{A2}A)\,A,\\
F_B' &= \theta\xi\gamma A - \frac{S\xi\gamma}{\mu_{M_B}} A F_B - \mu_{F_B} F_B,\\
B' &= \frac{S\xi\gamma}{\mu_{M_B}} A F_B + a_H R_H + a_V R_V - bB - \mu_B B,\\
Q_H' &= b\omega B - \tau_H H Q_H - \mu_{Q_H} Q_H,\\
Q_V' &= b(1-\omega)B - \tau_V V Q_V - \mu_{Q_V} Q_V,\\
R_H' &= p\tau_H H Q_H - a_H R_H - \mu_{R_H} R_H,\\
R_V' &= q\tau_V V Q_V - a_V R_V - \mu_{R_V} R_V.
\end{aligned} \tag{6}$$

2. The other natural assumption is that male and young female dynamics are fast. We argue, as in the previous case, that to prevent both populations from becoming extinct, we need to have also fast recruitment rates, so we assume that ξ is large, but here, there is no need to change the sex differentiation factor θ. Thus, we re-label the parameters as $\epsilon\hat{\mu}_{M_B} = \mu_{M_B}$, $\epsilon\hat{\mu}_{F_B} = \mu_{F_B}$ and $\epsilon\hat{\xi} = \xi$, where ϵ is a small positive parameter, $\hat{\theta} = \theta$ and $\theta, \mu_{M_B}, \mu_{F_B}$ and ξ are $O(1)$. Hence, the slow manifold is given by

$$M_B = \frac{(1-\theta)\xi\gamma A}{\mu_{M_B}}, \quad F_B = \frac{\theta\xi\gamma A}{\mu_{F_B}} \tag{7}$$

and the reduced system is

$$\begin{aligned}
A' &= \Lambda(R_H, R_V)\left(1 - \frac{A}{L_P}\right) - (\gamma + \mu_{A1} + \mu_{A2}A)\,A,\\
B' &= \frac{S\theta\,(1-\theta)\,\xi^2\gamma^2}{\mu_{M_B}\mu_{F_B}} A^2 + a_H R_H + a_V R_V - bB - \mu_B B,\\
Q_H' &= b\omega B - \tau_H H Q_H - \mu_{Q_H} Q_H,\\
Q_V' &= b(1-\omega)B - \tau_V V Q_V - \mu_{Q_V} Q_V,\\
R_H' &= p\tau_H H Q_H - a_H R_H - \mu_{R_H} R_H,\\
R_V' &= q\tau_V V Q_V - a_V R_V - \mu_{R_V} R_V.
\end{aligned} \tag{8}$$

We observe that (5) amounts to a biologically reasonable assumption that the newly emerging males are proportional to the existing biomass at a given time. Similarly, (7) translates into the assumption that females and males hatch in the numbers proportional to the current aquatic biomass. We note that such an assumption for the female population was used in [40]; similarly, in [47], it is assumed that the ratio of male and female offspring produced by a female is constant. The advantage of the multiscale approach is that it explicitly gives us the proportionality constants. We also note that we can exploit other possible fast processes, e.g., assuming the additional high female death rate due to the dangers of mating, which leads to even smaller systems with similar dynamics. Such models, which can also be derived from first principles, are discussed in [6]. Here, we shall focus on (5) and (6) as the analysis of (7), (8) can be carried out in the same way.

3. **Analysis of (6).** In this section, we shall analyse the dynamics of (6). Our approach uses extensively the theory of monotone, or cooperative, systems the necessary facts of which can be found in, e.g., [36, 37, 38] or [5, Chapter 8]. To avoid possible confusion, we begin with relevant notation. We denote open and closed positive cones in $\mathbb{R}^7$ by

$$\mathbb{R}^n_+ = (0,\infty)^n, \quad \overline{\mathbb{R}}^n_+ = [0,\infty)^n.$$

The latter introduces a partial order in $\mathbb{R}^n$. Accordingly, for any $\boldsymbol{a}, \boldsymbol{b} \in \mathbb{R}^n$, we write (i) $\boldsymbol{a} \leq \boldsymbol{b}$ when $a_i \leq b_i$, (ii) $\boldsymbol{a} < \boldsymbol{b}$ when $a_i \leq b_i$ and $\boldsymbol{a} \neq \boldsymbol{b}$, (iii) $\boldsymbol{a} \ll \boldsymbol{b}$ when $a_i < b_i$, where $i = 1, \ldots, n$. For $\boldsymbol{a} \leq \boldsymbol{b}$, we introduce order intervals

$$[\boldsymbol{a}, \boldsymbol{b}] = \{\boldsymbol{x} \in \mathbb{R}^n : \boldsymbol{a} \leq \boldsymbol{x} \leq \boldsymbol{b}\},$$

and for $\boldsymbol{a} \ll \boldsymbol{b}$,

$$[\boldsymbol{a}, \boldsymbol{b}) = \{\boldsymbol{x} \in \mathbb{R}^n : \boldsymbol{a} \leq \boldsymbol{x} \ll \boldsymbol{b}\}.$$

For future use, denote

$$\begin{gathered}
\boldsymbol{x} = (A, F_B, B, Q_H, Q_V, R_H, R_V), \quad \mathring{\boldsymbol{x}} = \left(\mathring{A}, \mathring{F}_B, \mathring{B}, \mathring{Q}_H, \mathring{Q}_V, \mathring{R}_H, \mathring{R}_V\right) \\
\alpha = \frac{S\xi\gamma}{\mu_{M_B}}, \quad l = L_P^{-1}, \quad \sigma_H = \tau_H H, \quad \sigma_V = \tau_V V, \quad T_B = b + \mu_B, \\
T_{Q_H} = \mu_{Q_H} + \sigma_H, \quad T_{Q_V} = \mu_{Q_V} + \sigma_V, \quad T_{R_H} = \mu_{R_H} + a_H, \quad T_{R_V} = \mu_{R_V} + a_V.
\end{gathered} \tag{9}$$

Lemma 3.1. *Consider the system represented by (6) and let $\lambda : [0,\infty) \to [0,\infty)$ be any oviposition rate. Then the flow of (6) is positively invariant on the set*

$$\Omega = \left\{\boldsymbol{x} \in \overline{\mathbb{R}}^7_+ : 0 \leq A \leq L_P,\ 0 \leq F_B \leq \frac{\theta\mu_{M_B}}{S}\right\}. \tag{10}$$

Proof. The positivity follows as the off-diagonal terms in (6) are nonnegative for nonnegative $\boldsymbol{x}$, [38, Theorem B.7]. The other bounds follow from the fact that $A'(L_P) < 0$ and $F_B'\left(\frac{\theta\mu_B}{S}\right) < 0$. □

Theorem 3.2. *Assume that the partial derivatives $\Lambda_{R_H}(R_H, R_Q)$ and $\Lambda_{R_Q}(R_H, R_Q)$ are nonnegative on $\overline{\mathbb{R}}^2_+$. Then (6) is a cooperative system on Ω.*

Proof. Let

$$\mathcal{J}(\boldsymbol{x}) = \begin{pmatrix}
J_{11} & 0 & 0 & 0 & 0 & (1-lA)\Lambda_{R_H} & (1-lA)\Lambda_{R_V} \\
J_{21} & J_{22} & 0 & 0 & 0 & 0 & 0 \\
\alpha F_B & \alpha A & -T_B & 0 & 0 & a_H & a_V \\
0 & 0 & b\omega & -T_{Q_H} & 0 & 0 & 0 \\
0 & 0 & b(1-\omega) & 0 & -T_{Q_V} & 0 & 0 \\
0 & 0 & 0 & p\sigma_H & 0 & -T_{R_H} & 0 \\
0 & 0 & 0 & 0 & q\sigma_V & 0 & -T_{R_V}
\end{pmatrix}, \tag{11}$$

where

$$J_{11} = -\mu_{\mathrm{A1}} - \gamma - 2A\mu_{\mathrm{A2}} - l\Lambda(R_H, R_V), \quad J_{21} = \gamma\xi\theta - \alpha F_B, \quad J_{22} = -\alpha A - \mu_{F_B}, \tag{12}$$

be the Jacobian matrix of (6). By (10) and the assumption, $J_{21} \geq 0$, $(1-lA)\Lambda_{R_H} \geq 0$ and $(1-lA)\Lambda_{R_V} \geq 0$, so that $\mathcal{J}(\boldsymbol{x})$ is a Metzler matrix on Ω and hence (6) is cooperative, [38, Theorem C.1]. □

Remark 3.3. The typical forms of λ satisfying the assumption of Theorem 3.2 are $\lambda(R) = \lambda_0$ for some constant λ_0, see [2, 15, 30] or a Holing type function with $a_H = a_V = a$

$$\Lambda(R) = \lambda_0 a \frac{R}{c+R},$$

see, e.g., [28]. Indeed, for $i = H, V$,

$$\Lambda_{R_i}(R_H, R_V) = \lambda_0 \frac{ac}{(c+R)^2} \geq 0.$$

In the first case, the per capita oviposition rate is unaffected by the overcrowding, but the pond's carrying capacity constrains the growth of the resulting aquatic forms, so the aquatic population cannot exceed L_P irrespective of the number of ovipositing females. On the other hand, the Holling type rate models the situation when the average per capita oviposition rate decreases with overcrowding, but the total number of laid eggs does not decrease to zero.

For the rest of this work, we shall assume that the mosquito population belongs to Ω. To proceed with the analysis, we assume that

$$\Lambda(R_H, R_A) = \lambda_0(a_H R_H + a_V R_V). \tag{13}$$

Next, we consider the existence of equilibria. The equation for equilibria can be written as

$$\begin{aligned} 0 &= \Lambda(R_H, R_V)\,(1 - lA) - (\gamma + \mu_{A1} + \mu_{A2} A)\,A, \\ 0 &= \theta\xi\gamma A - \alpha A F_B - \mu_{F_B} F_B, \\ 0 &= \mathcal{L}\boldsymbol{y} + \boldsymbol{G}, \end{aligned} \tag{14}$$

where

$$\mathcal{L} = \begin{pmatrix} -T_B & 0 & 0 & a_H & a_V \\ b\omega & -T_{Q_H} & 0 & 0 & 0 \\ b(1-\omega) & 0 & -T_{Q_V} & 0 & 0 \\ 0 & p\sigma_H & 0 & -T_{R_H} & 0 \\ 0 & 0 & q\sigma_V & 0 & -T_{R_V} \end{pmatrix}, \quad \boldsymbol{y} = \begin{pmatrix} B \\ Q_H \\ Q_V \\ R_H \\ R_H \end{pmatrix}, \quad \boldsymbol{G} = \begin{pmatrix} \alpha A F_B \\ 0 \\ 0 \\ 0 \\ 0 \end{pmatrix}.$$

We have

$$F_B^*(A) = \frac{\theta\xi\gamma A}{\mu_{F_B} + \alpha A}$$

and, using the fact that $\mathcal{L}$ is a nonsigular Metzler matrix,

$$\boldsymbol{y}^*(A) = -\mathcal{L}^{-1} \begin{pmatrix} \frac{\theta\xi\gamma\alpha A^2}{\mu_{F_B}+\alpha A} \\ 0 \\ 0 \\ 0 \\ 0 \end{pmatrix} =: -\mathcal{L}^{-1} \begin{pmatrix} f \\ 0 \\ 0 \\ 0 \\ 0 \end{pmatrix},$$

and the coordinates of

$$b(A) := (F_B^*(A), \boldsymbol{y}^*(A)) \tag{15}$$

are increasing functions of A. In particular,

$$F_B^*(A) \leq \lim_{A\to\infty} \frac{\theta\xi\gamma A}{\mu_{F_B} + \alpha A} = \frac{\theta\xi\gamma}{\alpha} = \frac{\theta\mu_{M_B}}{S}.$$

To derive the equation for A^*, we need parameters related to $\mathcal{L}^{-1}$. First,

$$\mathsf{L} := \det\mathcal{L} = T_{R_H} T_{R_V} T_{Q_H} T_{Q_V} T_B(\mathcal{R} - 1),$$

where

$$\begin{aligned}\mathcal{R} :=& \frac{b}{b+\mu_B}\left(\frac{(1-\omega)qa_V}{a_V+\mu_{R_V}}\frac{\tau_V V}{\tau_V V+\mu_{Q_V}}+\frac{\omega p a_H}{a_H+\mu_{R_H}}\frac{\tau_H H}{\tau_H H+\mu_{Q_H}}\right)\\ =& \frac{b}{T_B}\left(\frac{(1-\omega)qa_V}{T_{R_V}}\frac{\sigma_V}{T_{Q_V}}+\frac{\omega p a_H}{T_{R_H}}\frac{\sigma_H}{T_{Q_H}}\right)\end{aligned}$$

gives the average number of reproducing females produced from one breeding female. We observe that in this model, we have $\mathcal{R}<1$. Then,

$$\begin{aligned}R_H &= -f\frac{bT_{R_V}T_{Q_V}\omega p a_H\sigma_H}{a_H \mathsf{L}} = f\frac{b\omega p a_H\sigma_H}{a_H T_{R_H}T_{Q_H}T_B(1-\mathcal{R})}\\ R_V &= -f\frac{bT_{R_H}T_{Q_H}(1-\omega)qa_V\sigma_V}{a_V \mathsf{L}} = f\frac{b(1-\omega)qa_V\sigma_V}{a_V T_{R_V}T_{Q_V}T_B(1-\mathcal{R})}.\end{aligned} \tag{16}$$

Hence,

$$a_H R_H + a_V R_V = f\frac{\mathcal{R}}{1-\mathcal{R}}, \tag{17}$$

and further

$$B = f\frac{1}{(b+\mu_B)(1-\mathcal{R})},\quad Q_H = f\frac{b\omega}{T_{Q_H}T_B(1-\mathcal{R})},\quad Q_V = f\frac{b(1-\omega)}{T_{Q_V}T_B(1-\mathcal{R})}. \tag{18}$$

We shall need

$$\rho\mathcal{D} := \frac{\lambda_0\theta\xi\gamma}{\mu_{A_2}}\mathcal{D} = \frac{\lambda_0\theta\xi\gamma}{\mu_{A_2}}\frac{\mathcal{R}}{1-\mathcal{R}}, \tag{19}$$

and

$$\Gamma := \frac{\gamma+\mu_{A1}}{\mu_{A2}},\quad \Delta := \frac{\mu_{F_B}}{\alpha}.$$

Then, substituting (17) into the first equation of system (14), after some algebra, we obtain the equation determining the equilibrium values of A as

$$A\left((l\rho\mathcal{D}+1)A^2+(\Gamma+\Delta-\rho\mathcal{D})A+\Gamma\Delta\right)=0. \tag{20}$$

To analyze the nonzero equilibrium values, we see that at any non-zero equilibrium of A we have

$$\rho\mathcal{D} = \frac{A^2+(\Gamma+\Delta)A+\Gamma\Delta}{A(1-lA)} =: F(A),\quad 0<A<L_P.$$

We see that $\lim_{A\to 0,l^{-1}} F(A)=\infty$ and $F(A)$ is monotonically decreasing on $(0,A_{12})$ and monotonically increasing on (A_{12},l^{-1}), where the minimum of F is given by

$$A_{12} = \frac{l\Gamma\Delta+\sqrt{l^2\Gamma^2\Delta^2+\Gamma\Delta+\Gamma\Delta(1+(\Gamma+\Delta)l)}}{1+(\Gamma+\Delta)l}.$$

We define

$$N^* = F(A_{12}),$$

and let A_1 and A_2 be, respectively, the smaller and the larger root of $F(A)=\rho\mathcal{D}$ if $\rho\mathcal{D}>N^*$.

To find N^*, it is easier to use the fact that for $\rho\mathcal{D}=N^*$, the quadratic equation in (20) has one double root, that is, its discriminant must be zero. This gives

$$N^* = \Gamma+\Delta+2l\Gamma\Delta+2\sqrt{\Gamma\Delta+l(\Gamma+\Delta)\Gamma\Delta+l^2\Gamma^2\Delta^2}$$

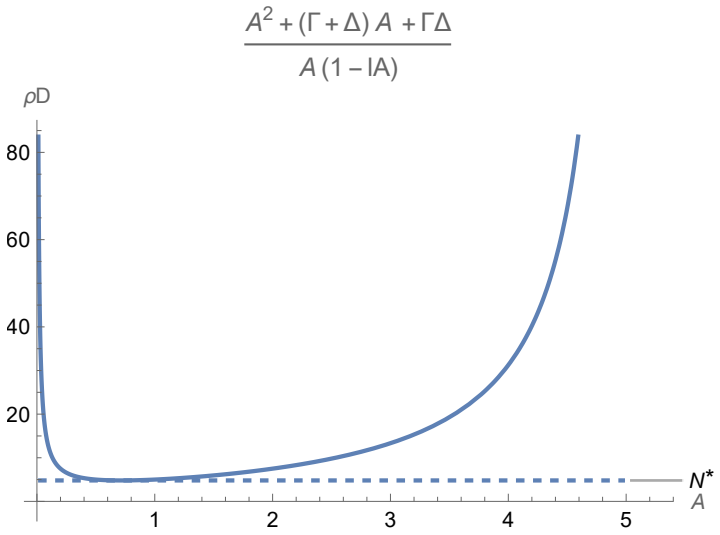

FIGURE 2. Saddle-node bifurcation in the model.

In the special case $l = 0$,

$$N^* = \left(\sqrt{\Gamma} + \sqrt{\Delta}\right)^2, \quad A_{12} = \sqrt{\Gamma\Delta}. \tag{21}$$

We define

$$\boldsymbol{x}(A) = (A, b(A)).$$

We can now summarize our considerations in the following theorem.

Theorem 3.4 (Existence of Steady State Solutions)**.** *1. If $\rho\mathcal{D} < N^*$, then there is only a trivial steady state.*

2. If $\rho\mathcal{D} = N^*$, then the trivial steady state coexists with one strictly positive steady state $\boldsymbol{x}(A_{12}) \gg \mathbf{0}$.

3. If $\rho\mathcal{D} > N^*$, then there are the trivial steady state and two strictly positive steady states $\boldsymbol{x}(A_2) \gg \boldsymbol{x}(A_1) \gg \mathbf{0}$.

Furthermore, for $\rho\mathcal{D} > N^*$, $A_1(\rho\mathcal{D})$ monotonically decreases from A_{12} to 0 and $A_2(\rho\mathcal{D})$ monotonically increases from A_{12} to L_P as $\rho\mathcal{D}$ increases from N^* to ∞. Thus, the smaller equilibrium $\boldsymbol{x}(A_1)$ monotonically decreases to $\mathbf{0}$ and the larger equilibrium $\boldsymbol{x}(A_2)$ monotonically increases to $(L_p, b(L_P))$ as $\rho\mathcal{D} \to \infty$.

Remark 3.5. The threshold condition $\rho\mathcal{D} \lessgtr N^*$ can be written as

$$\mathcal{R} \lessgtr \frac{N^*}{\rho + N^*} < 1,$$

where the right-hand side contains only parameters of the pre-mating stages and $\mathcal{R}$ depends only on the post-mating ones. Hence, increasing the productivity of breeding females allows a positive equilibrium to appear. Similarly, if we increase the oviposition rate λ_0, see (19), we observe the same effect.

Next, we shall focus on the stability of the steady states. The results are similar to that obtained in [40] in a structurally similar 3-dimensional case. To continue,

we define the point

$$\boldsymbol{\eta} = \left(L_P, \frac{\theta\mu_B}{S}, B^0, Q_H^0, Q_V^0, R_H^0, R_V^0\right) = \left(L_P, \frac{\theta\mu_B}{S}, \boldsymbol{y}^0\right),$$
$$\text{with } \boldsymbol{y}^0 = -\mathcal{L}^{-1}\begin{pmatrix} \theta\xi\gamma L_P \\ 0 \\ 0 \\ 0 \\ 0 \end{pmatrix}. \tag{22}$$

We see that $\boldsymbol{\eta} \in \Omega$, hence $[\mathbf{0}, \boldsymbol{\eta}] \subset \Omega$.

Theorem 3.6. *Suppose (13) holds and $\rho\mathcal{D} < N^*$, where N^* is defined by (21). Then, the trivial steady state is globally asymptotically stable on Ω.*

Proof. The proof uses [2, Theorem 6] or [36, Proposition 5.8.2], see also [5, Theorem 8.30]. Let us write (6) as

$$\boldsymbol{x}' = \boldsymbol{f}(\boldsymbol{x}). \tag{23}$$

We have $\boldsymbol{f}(\boldsymbol{\eta}) = \left(-(\gamma + \mu_{A1} + \mu_{A2}L_P)L_P, -\frac{\mu_{F_B}\theta\mu_B}{S}, 0, 0, 0, 0, 0\right)$. By (16) and (18) with $f = \theta\xi\gamma L_P$, we have $\boldsymbol{\eta} \gg \mathbf{0}$. Further, $\boldsymbol{f}(\boldsymbol{\eta}) < \mathbf{0}$ and $\boldsymbol{f}(\mathbf{0}) = \mathbf{0}$. Since, by assumption and Theorem 3.4, the trivial steady state is the only steady state in $[\mathbf{0}, \boldsymbol{\eta}]$, we conclude that the trivial steady state is globally and asymptotically stable in $[\mathbf{0}, \boldsymbol{\eta}]$, see [2] or [5, Theorem 8.30].

Next, for any $m \in \mathbb{N}$, we define

$$\boldsymbol{\eta}_m = \left(L_P, \frac{\theta\mu_B}{S}, m\boldsymbol{y}^0\right). \tag{24}$$

Then, since

$$\theta\xi\gamma L_P + a_H R_H + a_V R_V - bB - \mu_B B = 0,$$

we get

$$a_H R_H + a_V R_V - bB - \mu_B B < 0.$$

Hence,

$$\theta\xi\gamma L_P + ma_H R_H + ma_V R_V - mbB - m\mu_B B < 0,$$

and therefore

$$\mathcal{L}\boldsymbol{\eta}_m + \begin{pmatrix} \theta\xi\gamma L_P \\ 0 \\ 0 \\ 0 \\ 0 \end{pmatrix} \leq \mathbf{0}.$$

Thus, $\boldsymbol{f}(\boldsymbol{\eta}_m) \leq \mathbf{0}$ for any $m \in \mathbb{N}$ and therefore $\mathbf{0}$ is globally asymptotically stable on Ω. □

We precede the analysis of the $\rho\mathcal{D} \geq N^*$ case with the following lemma.

Lemma 3.7. *Suppose (13) holds and $\rho\mathcal{D} > N^*$. There exist points $\boldsymbol{y}, \boldsymbol{z}$ in Ω such that $\mathbf{0} \ll \boldsymbol{y} \ll \boldsymbol{x}^*(A_1) \ll \boldsymbol{z} \ll \boldsymbol{x}^*(A_2)$, $\boldsymbol{f}(\boldsymbol{y}) < \mathbf{0}$ and $\boldsymbol{f}(\boldsymbol{z}) > \mathbf{0}$.*

Proof. Steady states of (6) are obtained by solving (14). Dropping the first equation of (14), we get

$$\begin{aligned} 0 &= \theta\xi\gamma A - \alpha A F_B - \mu_{F_B} F_B, \\ 0 &= \mathcal{L}\boldsymbol{y} + \boldsymbol{G}. \end{aligned} \tag{25}$$

For each $A \in [0, L_P]$, we consider the point $\boldsymbol{b}(A)$ defined in (15). If $A = A_1$ or $A = A_2$, then $(A_i, \boldsymbol{b}(A_i))$, $i = 1, 2$, is a steady state of (6). To ensure that this is not the case, we consider the first equation of (14) and solve for A the inequality

$$-AP_2(A) > 0, \tag{26}$$

where $P_2(A)$ the quadratic polynomial in (20). Since $A > 0$, we see that

1. $-AP_2(A) > 0$ if and only if $A \in (A_1, A_2)$ and
2. $-AP_2(A) < 0$ if and only if $A \in (0, A_1) \cup (A_2, L_P]$.

To complete the proof, we define $\boldsymbol{y} = (y, \boldsymbol{b}(y))$ and $\boldsymbol{z} = (z, \boldsymbol{b}(z))$, where y is any point in $(0, A_1)$ and z is any point in (A_1, A_2) and apply the fact that $b(A)$ is a strictly increasing function of A. □

Theorem 3.8. *Suppose (13) holds.*

1. *Let $\rho\mathcal{D} > N^*$. Then $[\mathbf{0}, \boldsymbol{x}^*(A_1)]$ and $\{\boldsymbol{x} \in \Omega : \boldsymbol{x} \geq \boldsymbol{x}^*(A_1)\}$ are positively invariant and the steady states $\mathbf{0}$ and $\boldsymbol{x}^*(A_2)$ are globally asymptotically stable on, respectively, $[\mathbf{0}, \boldsymbol{x}^*(A_1)] \setminus \{\boldsymbol{x}^*(A_1)\}$ and $\{\boldsymbol{x} \in \Omega : \boldsymbol{x} > \boldsymbol{x}^*(A_1)\}$.*
2. *Let $\rho\mathcal{D} = N^*$. Then $[\mathbf{0}, \boldsymbol{x}^*(A_{12})]$ and $\{\boldsymbol{x} \in \Omega : \boldsymbol{x} \geq \boldsymbol{x}^*(A_{12})\}$ are positively invariant and the steady states $\mathbf{0}$ and $\boldsymbol{x}^*(A_{12})$ are globally asymptotically stable on, respectively, $[\mathbf{0}, \boldsymbol{x}^*(A_{12})] \setminus \{\boldsymbol{x}^*(A_{12})\}$ and $\{\boldsymbol{x} \in \Omega : \boldsymbol{x} > \boldsymbol{x}^*(A_{12})\}$.*

Proof. Consider statement 1. The invariance of $[\mathbf{0}, \boldsymbol{x}^*(A_1)]$ follows directly from [5, Theorem 8.30]. Using the same result, we see that $[\mathbf{0}, \boldsymbol{\eta}_m]$, where $\boldsymbol{\eta}_m$ was defined in (24), is invariant, and we obtain the invariance of $\{\boldsymbol{x} \in \Omega : \boldsymbol{x} \geq \boldsymbol{x}^*(A_1)\}$ by passing with m to ∞.

Now, let the points $\boldsymbol{y}$ and $\boldsymbol{z}$ be as constructed in the proof of Lemma 3.7. We can make $\boldsymbol{y}$ as close to A_1 as we wish, and thus $b(\boldsymbol{y}) \ll \boldsymbol{x}^*(A_1)$ can be arbitrarily close coordinatewise to $\boldsymbol{x}^*(A_1)$. Since $\boldsymbol{f}(\boldsymbol{y}) < \mathbf{0}$, $\mathbf{0}$ is globally asymptotically stable on $[\mathbf{0}, \boldsymbol{x}^*(A_1))$.

Moreover, for sufficiently large m, we have $\boldsymbol{x}^*(A_1) \ll \boldsymbol{z} \ll \boldsymbol{x}^*(A_2) \ll \boldsymbol{\eta}_m$, with $\boldsymbol{f}(\boldsymbol{\eta}_m) < 0$ and $b(\boldsymbol{z})$ can be chosen arbitrarily close to $\boldsymbol{x}^*$. Thus, $\boldsymbol{x}^*(A_2)$ is globally asymptotically stable on $\{\boldsymbol{x} \in \Omega : \boldsymbol{x} \gg \boldsymbol{x}^*(A_1)\}$.

To shorten notation, we denote

$$\boldsymbol{x}^*(A_1) = \boldsymbol{x}^* = (x_1^*, \ldots, x_7^*)$$

and show that the stability can be extended to the faces

$$\begin{aligned} I_i &= \{\boldsymbol{x} : x_i = x_i^*, 0 \leq x_j \leq x_j^*\} \setminus \{\boldsymbol{x}^*\}, \quad j = 1, \ldots, 7, \\ J_i &= \{\boldsymbol{x} \in \Omega : x_i = x_i^*, x_j \geq x_j^*\} \setminus \{\boldsymbol{x}^*\}, \quad j = 1, \ldots, 7. \end{aligned} \tag{27}$$

We observed that both sets $[\mathbf{0}, \boldsymbol{x}^*(A_1)]$ and $\{\boldsymbol{x} \in \Omega : \boldsymbol{x} \geq \boldsymbol{x}^*(A_1)\}$ are invariant. We can directly check that no face (27) is invariant. Indeed, consider first I_1. Then $f_1(x_1^*, x_6, x_7) < 0$ if $0 < x_6 < x_6^*$ or $0 < x_7 < x_7^*$ and thus the only invariant part of I_1 can be $x_1 = x_1^*, x_6 = x_6^*$ and $x_7 = x_7^*$. But then $f_6(x_4, x_6^*) < 0$ or $f_7(x_5, x_7^*) < 0$ unless $x_4 = x_4^*$ and $x_5 = x_5^*$. Hence, the only invariant subset can be $x_1 = x_1^*, x_4 = x_4^*, x_5 = x_5^*, x_6 = x_6^*, x_7 = x_7^*$. Then, however, $f_4(x_3, x_5^*) < 0$ or $f_5(x_3, x_5^*) < 0$ unless $x_3 = x_3^*$. Arguing as above, $f_3(x_1^*, x_2, x_3^*, x_6^*, x_7^*) < 0$ unless $x_2 = x_2^*$. But then we are at x^*. The other $I_i's$ and $J_i's, i = 1, \ldots, 7$, follow in an analogous way.

Hence, trajectories originating from the faces must enter the interior of the respective order intervals and thus converge to the equilibria in them.

To prove 2., we observe that we can repeat the above considerations for $A_{12} = A_1 = A_2$. □

A standard monotonicity argument gives the following.

Corollary 3.9. *Let $\rho\mathcal{D} > N^*$. Then $[\mathbf{0}, \boldsymbol{x}^*(A_2)]$ is invariant and globally attractive in Ω.*

Proof. The first statement follows as in the proof of statement 1 of Theorem 3.8, [5, Theorem 8.30], since $\boldsymbol{f}(\mathbf{0}) = \boldsymbol{f}(\boldsymbol{x}^*(A_2)) = \mathbf{0}$. For the second, we observe that for any $\boldsymbol{y} \in \Omega$, we can find $\boldsymbol{z} \in \{\boldsymbol{x} \in \Omega, \boldsymbol{x} > \boldsymbol{x}^*(A_1)\}$ such that $\boldsymbol{y} \leq \boldsymbol{z}$, the respective solutions satisfy $\mathbf{0} \leq \boldsymbol{\phi}(t, \boldsymbol{y}) \leq \boldsymbol{\phi}(t, \boldsymbol{z}), t \geq 0$ and, since $\lim_{t\to\infty} \boldsymbol{\phi}(t, \boldsymbol{z}) = \boldsymbol{x}^*(A_2)$, the $\omega-$limit set of $\phi(t, \boldsymbol{y})$ satisfies $\omega_{\boldsymbol{y}} \in [\mathbf{0}, \boldsymbol{x}^*(A_2)]$. □

Corollary 3.10. *Under assumptions of Theorem 3.8 1., the steady state $\boldsymbol{x}^*(A_1)$ is unstable. If the assumptions of Theorem 3.8 2. are satisfied, the steady state $\boldsymbol{x}^*(A_{12})$ is unstable.*

Proof. In both cases, the steady states do not attract trajectories of the order interval extending from $\mathbf{0}$ to them. □

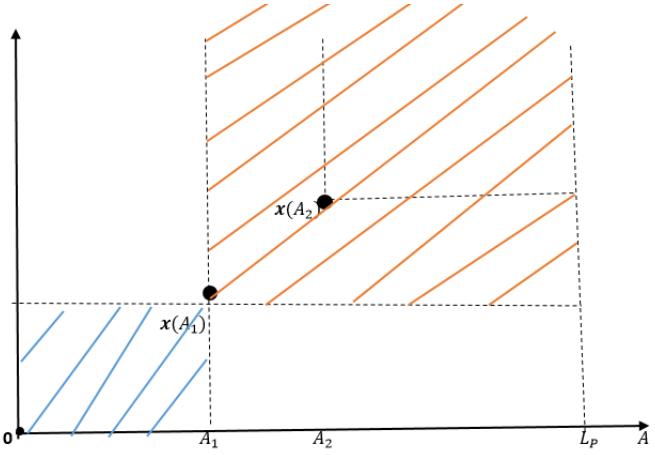

FIGURE 3. 2-dimensional representation of the case $N > N^*$. The horizontal axis represents the aquatic lifeforms, while all other coordinates are combined on the vertical axis. The box shaded in orange represents the basin of attraction for the steady state $\boldsymbol{x}^*(A_2)$, while the box shaded in blue represents the basin of attraction of the trivial steady state.

4. **Asymptotic equivalence of the dynamics.** To formulate the result on the equivalence of dynamics of (4) and (6), we first introduce the necessary notation. Let

$$\boldsymbol{x}_\epsilon(t) := (A_\epsilon(t), M_{B,\epsilon}(t), F_{B,\epsilon}(t), B_\epsilon(t), Q_{H,\epsilon}(t), Q_{V,\epsilon}(t), R_{H,\epsilon}(t), R_{V,\epsilon}(t))$$

be the solution to (4) with the initial condition $\boldsymbol{x}_\epsilon(0) = \hat{\boldsymbol{x}}$, and

$$\boldsymbol{x}_0(t) := (A_0(t), F_{B,0}(t), B_0(t), Q_{H,0}(t), Q_{V,0}(t), R_{H,0}(t), R_{V,0}(t)),$$

be the solution to (6) with $\boldsymbol{x}_0(0) = (\mathring{A}, \mathring{F}_B, \mathring{B}, \mathring{Q}_H, \mathring{Q}_V, \mathring{R}_H, \mathring{R}_V)$, and

$$M_{B,0}(t) = \frac{\xi\gamma}{\mu_{M_B}} A_0(t).$$

We have

Theorem 4.1. *Let*

$$(\mathring{A}, \mathring{F}_B, \mathring{B}, \mathring{Q}_H, \mathring{Q}_V, \mathring{R}_H, \mathring{R}_V) \in \begin{cases} \Omega & \text{for} \quad \mathcal{D} < \rho^{-1}N^*, \\ ([\mathbf{0}, \boldsymbol{x}(A^*)] \setminus \{\boldsymbol{x}(A^*)\}) \cup \{\boldsymbol{x} \in \Omega : \boldsymbol{x} > \boldsymbol{x}(A^*)\} & \text{for} \quad \mathcal{D} \geq \rho^{-1}N^*, \end{cases}$$

where $A^* = A_1$ *if* $\mathcal{D} > \rho^{-1}N^*$ *and* $A^* = A_{12}$ *if* $\mathcal{D} = \rho^{-1}N^*$, *and* $\mathring{M}_B \geq 0$ *be arbitrary. Then*

$$(A_\epsilon(t), F_{B,\epsilon}(t), B_\epsilon(t), Q_{H,\epsilon}(t), Q_{V,\epsilon}(t), R_{H,\epsilon}(t), R_{V,\epsilon}(t)) = \boldsymbol{x}_0(t) + O(\epsilon), \quad \epsilon \to 0, \tag{28}$$

uniformly for $t \in [0, \infty)$, *and, for any* $t_0 > 0$,

$$M_{B,\epsilon}(t) = M_{B,0}(t) + O(\epsilon), \quad \epsilon \to 0, \tag{29}$$

uniformly for $t \in [t_0, \infty)$.

Before the proof, we note that (29) is valid only on intervals separated from zero because we have not included the initial layer to compensate for the fact that arbitrary initial conditions cannot satisfy (5). As explained in [4, 3], this can be easily remedied, but we skip this part to shorten the discussion.

Proof. The proof is a standard application of [4, Theorem 1 & Remark 3], see also [8, Appendices A & B]. It is easy to see that all assumptions of the classical Tikhonov theorem, [43], are satisfied, with (5) defining the only quasi-steady state whose all points are uniformly asymptotically stable equilibria of the fast equation $\frac{\tilde{M}_B}{d\tau} = \xi\gamma A - \mu_{M_B}\tilde{M}_B, \tau = t/\epsilon$, and any $\mathring{M}_B$ belongs to the basin of attraction of

$$\frac{\tilde{M}_B}{d\tau} = \xi\gamma\mathring{A} - \mu_{M_B}\tilde{M}_B \tag{30}$$

for any $\mathring{A}$ (see assumptions a)–d) of [8, Appendix A]). This gives the validity of the approximation (28) and (29) on bounded time intervals. To extend it to infinite intervals, we use [4, Remark 3], which ensures that it is possible for any $X_\epsilon(t)$ emanating from $(\mathring{A}, \mathring{M}_B, \mathring{F}_B, \mathring{B}, \mathring{Q}_H, \mathring{Q}_V, \mathring{R}_H, \mathring{R}_V)$ such that $(\mathring{A}, \mathring{F}_B, \mathring{B}, \mathring{Q}_H, \mathring{Q}_V, \mathring{R}_H, \mathring{R}_V)$ is in the domain of attraction of a (hyperbolic) equilibrium of (6), and $\mathring{F}_B$ is in the basin of attraction of equilibria of (30), that is, it is arbitrary. Then, e.g., [4, Theorem 1] ensures that $X_\epsilon(t)$ converges to

$$(A_0(t), M_{B,0}(t), F_{B,0}(t), B_0(t), Q_{H,0}(t), Q_{V,0}(t), R_{H,0}(t), R_{V,0}(t))$$

uniformly in t on any interval $[0, \infty)$, except for $M_B(t)$, which converges to $M_{B,0}(t)$ uniformly on $[t_0, 0)$ for any $t_0 > 0$.

To get the order of convergence in (28) and (29), we use the higher order result, [3, Theorem 3], and obtain the desired result by retaining only zero-order terms, as explained in [8, Theorem B.2]. □

Parameter	Range	Source \ Comment	Value used
μ_{M_B}	$\frac{1}{7} - \frac{1}{6}\ day^{-1}$	[41]	$\frac{1}{6}\ day^{-1}$
$\mu_X = \frac{1}{20}$ $X \in \{F_B, Q_H, Q_V, R_H, R_V\}$	$\frac{1}{28} - \frac{1}{14}\ day^{-1}$	[41]	$\frac{1}{20}\ day^{-1}$
γ	$\frac{1}{10} - \frac{1}{7}\ day^{-1}$ for *Aedes aegypti* or $\frac{1}{14} - \frac{1}{10}$ for *Anopheles* mosquitoes	[17]	$\frac{1}{10}\ day^{-1}$
L_P		Estimated	100000 A_q
b		[12]	$\frac{1}{3} day^{-1}$
p	0.70-0.95	[12, 29]	0.86
q		We assume $q \geq p$	0.95
ω		We assume that mosquitoes have a higher preference for human blood than for other vertebrates.	0.8
$\tau_H H, \tau_V V$		Estimated	$\tau_H = 1H^{-1}day^{-1}$ $\tau_V = 1.4V^{-1}day^{-1}$
a_H		[29]	$a_H = 1day^{-1}$
a_V		We assume that alternative blood sources are closer to breeding sites than humans, so $a_V > a_H$.	$a_V = 1.2day^{-1}$
μ_{A1}		Estimated	0.001 day^{-1}
μ_{A2}		Estimated	0.0002 $A_q^{-1}day^{-1}$
S		Estimated	0.0001 $M^{-1}T^{-1}$
θ		[35]	0.5
ξ		Estimated	1
λ_0		Bifurcation parameter	–

TABLE 3. Parameters used for numerical experiments presented in Figures 4, 5 and 6. Parameters such as $\tau_H H$, $\tau_V V$, ξ, μ_{A1}, μ_{A2}, L_P are estimated for the purpose of these simulations.

5. **Numerical Simulations.** Here, we numerically solve systems (6) and (4), and compare the results for different values of ϵ. Our approximations are good even for relatively large values $\epsilon = 0.3$, which means that the death rate of the males is about three times higher than that of the newly hatched females. This is quite reasonable since male mosquitoes typically live for 6 to 7 days while the females live for 14 to 28 days, [41].

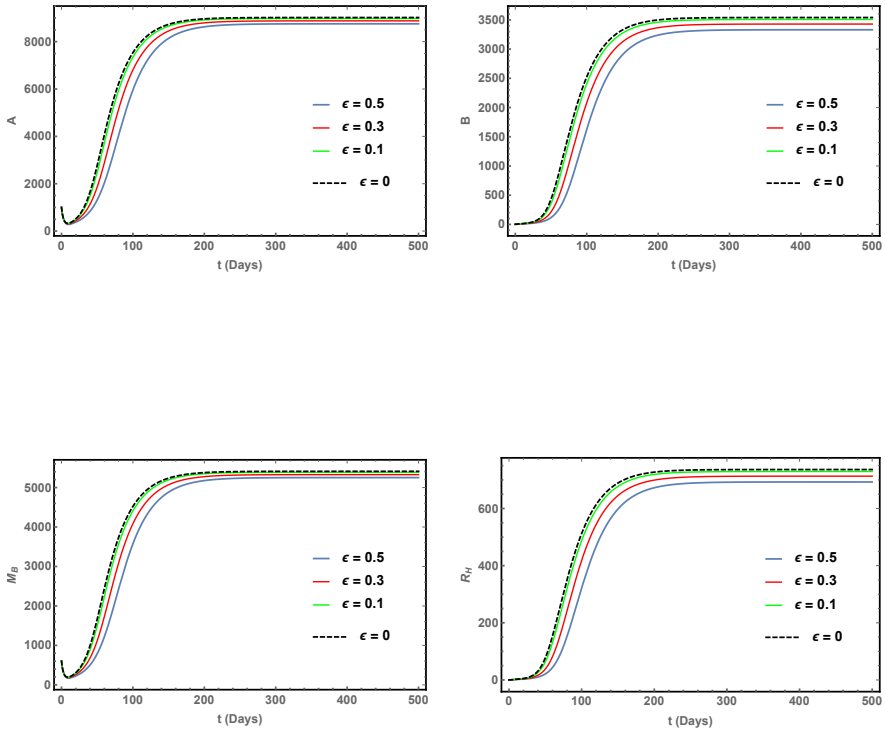

FIGURE 4. The parameter values used are defined in Table 3 with $\lambda_0 = 20$. $\rho\mathcal{D} = 11435.5 > N^* = 2652.86$, and we identify three steady-state solutions corresponding to $A^* = 0, A^* = 41.872$, and $A^* = 9019.09$. The steady-state $\boldsymbol{x}(9019.09)$ is stable, as demonstrated by the long-term behaviour of the trajectories. This figure shows the quality of approximation for initial conditions in the basin of attraction of the stable equilibrium $\boldsymbol{x}^*(9019.09)$ for different values of ϵ; the case $\epsilon = 0$ corresponds to the solution of (6).

6. **Conclusions.** In this paper, we considered an eight-stage model of a mosquito life cycle introduced in [31] and briefly compared it with several existing models describing similar scenarios, [2, 27, 28, 40, 47]. We used the model's multiscale character to explore possibilities of reducing its complexity using the quasi-steady state (QSS) approximation and provided its biological interpretation. Using recent results in asymptotic analysis, we show that for small scaling parameter values, the reduced model retains salient features of the original dynamics as long as the initial condition is in the basin of attraction of a (hyperbolic) equilibria of the reduced model. Moreover, numerical simulations show that the dynamics of the reduced

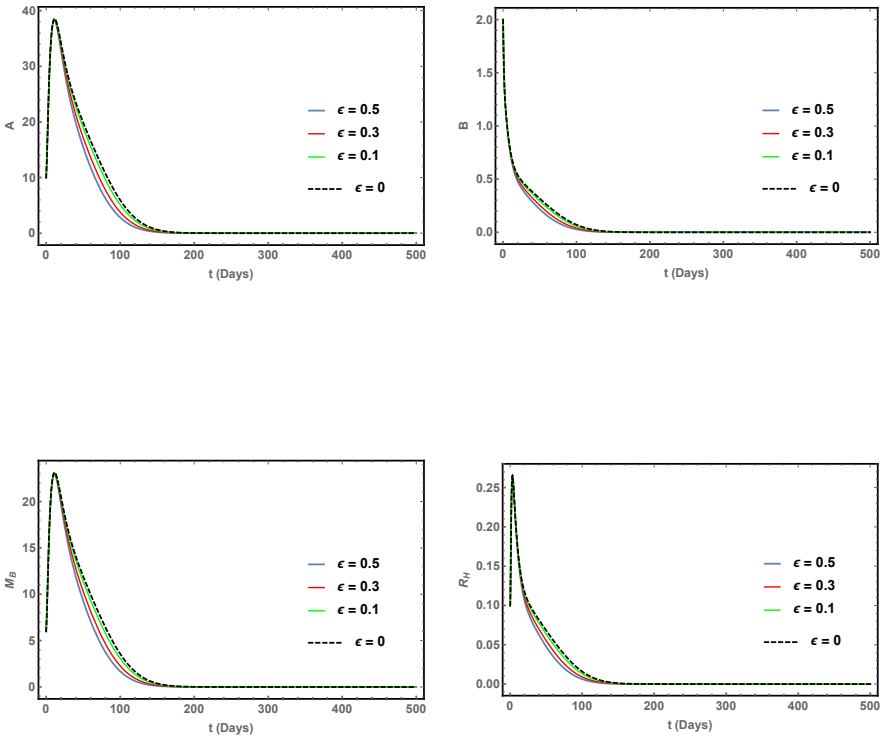

FIGURE 5. The parameter values used here are the same as those in Figure 4. Without altering these parameter values, we modify the initial conditions so that they fall within the basin of attraction of the trivial steady state. The trajectory for $\epsilon = 0$ corresponds to the solution of (6).

model agree well with that of the original system also for larger values of the scaling parameter, confirming the broader validity of the biological assumptions behind the QSS approximation. Since the latter is monotone, analysing its dynamics is relatively straightforward. In particular, we identify the bifurcation parameter, which nicely splits into two parts, one containing only post-mating parameters and the other involving only the parameters of the aquatic and the pre-mating stages. If the bifurcation parameter is below the explicitly evaluated threshold, only the trivial equilibrium, which is globally asymptotically stable, exists. When the bifurcation parameter crosses the threshold, we observe a saddle-node bifurcation, which has the additional feature that the two new equilibria are ordered (with respect to the partial order in $\overline{\mathbb{R}}^7_+$), with the smaller being unstable, and the trivial and the larger asymptotically stable, in the order intervals stretching from $\mathbf{0}$ to the smaller equilibrium and from the smaller equilibrium to the boundary of the feasible domain Ω, respectively. Thus, the dynamics of the model may exhibit a multidimensional Allee

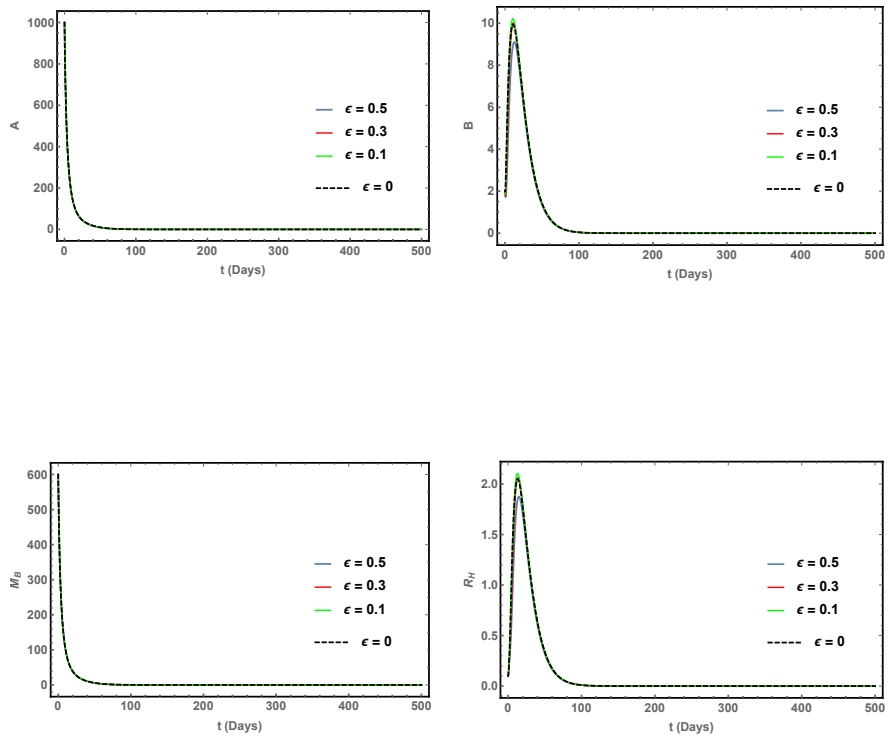

FIGURE 6. The parameter values used are defined in Table 3 with $\lambda_0 = 1$, $\rho\mathcal{D} = 571.773 < N^* = 2652.86$ so we only have the trivial steady state which is globally and asymptotically stable. The trajectory for $\epsilon = 0$ corresponds to the solution of (6).

effect, which is in agreement with results obtained for two- and three-dimensional models with similar structure in [22, 28, 40, 47]. In particular, when the bifurcation parameter (for instance, the number of laid eggs per capita λ_0) tends to infinity, the smaller equilibrium tends to zero, destabilizing thus the trivial equilibrium by shrinking its basin of attraction. In comparison, the larger equilibrium tends to the boundary of Ω, and thus, the larger equilibrium asymptotically becomes globally stable on Ω. Using asymptotic analysis, we show that these properties are also the features of the dynamics of the original problem. We realize that some assumptions used to obtain the results of this paper are a significant simplification of biological reality. Future work will be devoted to validating the conclusions presented here with experimental data. Another direction being pursued is a comprehensive analysis of lower-dimensional multistage mosquito life-cycle models aimed at the identification of possible sources leading to the emergence of the Allee effect and combining the models with human dynamics to build more comprehensive malaria models, extending thus the work such as [26].

REFERENCES

[1] R. Anguelov, C. Dufourd, and Y. Dumont. Mathematical model for pest-insect control using mating disruption and trapping. *Appl. Math. Model.*, 52:437–457, 2017.

[2] R. Anguelov, Y. Dumont, and J. Lubuma. Mathematical modeling of sterile insect technology for control of anopheles mosquito. *Computers & Mathematics with Applications*, 64(3):374–389, 2012.

[3] J. Banasiak. Some remarks on the renormalization group and Chapman-Enskog type methods in singularly perturbed problems. *Math. Methods Appl. Sci.*, 43(18):10361–10380, 2020.

[4] J. Banasiak. A note on the Tikhonov theorem on an infinite interval. *Vietnam J. Math.*, 49(1):69–86, 2021.

[5] J. Banasiak. *Introduction to Mathematical Methods in Population Theory*. Springer Verlag, 2024.

[6] J. Banasiak, B. M. Ghakanyuy, and G.A. Ngwa. Emergence and analysis of multidimensional Allee effect in mosquito life cycle. in preparation.

[7] J. Banasiak and M. Lachowicz. *Methods of small parameter in mathematical biology*. Springer, Heidelberg/New York, 2014.

[8] J. Banasiak and S.Y. Tchoumi. Multiscale malaria models and their uniform in-time asymptotic analysis. *Mathematics and Computers in Simulation*, 221:1–18, 2024.

[9] E. Beretta, V. Capasso, and D. G. Garao. A mathematical model for malaria transmission with asymptomatic carriers and two age groups in the human population. *Mathematical Biosciences*, 300:87–101, 2018.

[10] J. D. Charlwood and M. D. R. Jones. Mating behaviour in the mosquito *Anopheles gambiae s. l.* i. Close range and contact behaviour. *Physiological Entomology*, 4(2):111–120, 1979.

[11] J. D. Charlwood, R. Thompson, and H. Madsen. Observations on the swarming and mating behaviour of *Anopheles funestus* from southern Mozambique. *Malaria Journal*, 2(2):http://www.malariajournal.com/content/s/1/2, 2003.

[12] N. Chitnis, T. Smith, and R. Steketee. A mathematical model for the dynamics of malaria in mosquitoes feeding on a heterogeneous host population. *Journal of Biological Dynamics*, 2(3):259–285, 2008.

[13] A. N. Clements. *The biology of mosquitoes, Volume 1: Development, nutrition and reproduction*. Cabi GB, 2023.

[14] G. B. Craig Jr. Mosquito: female monogamy induced by a male accessory gland substance. *Science*, 156(781):1499–1501, 1967.

[15] Y. Dumont and J. Thuilliez. Human behaviors: A threat to mosquito control? *Mathematical Biosciences*, 281:9–23, 2016.

[16] X. Fauvergue. A review of mate-finding Allee effects in insects: from individual behavior to population management. *Entomologia Experimentalis et Applicata*, 146(1):79–92, 2013.

[17] Centers for Disease Control and Prevention. Mosquito life cycle, 2023. Accessed: 2025-02-05.

[18] B. M. Ghakanyuy, M. I. Teboh-Ewungkem, K. A. Schneider, and G. A. Ngwa. Investigating the impact of multiple feeding attempts on mosquito dynamics via mathematical models. *Mathematical Biosciences*, 350:108832, 2022.

[19] D. Goindin, Ch. Delannay, C. Ramdini, J. Gustave, and F. Fouque. Parity and longevity of aedes aegypti according to temperatures in controlled conditions and consequences on dengue transmission risks. *PloS one*, 10(8):e0135489, 2015.

[20] L. Gomulski. Polyandry in nulliparous *Anopheles gambiae* mosquitoes (diptera: Culicidae). *Bullettin of Entomological Research*, 80(4):393–396, 1990.

[21] G. Hek. Geometric singular perturbation theory in biological practice. *Mathematical Biology*, 60:347–386, 2010.

[22] L. Hong, Y. Yang, W. Zhang, M. Huang, and X. Zhou. Study on discrete mosquito population-control models with Allee effect. *Axioms*, 14(3):193, 2025.

[23] F. Ch. Hoppensteadt. Singular perturbations on the infinite interval. *Trans. Amer. Math. Soc.*, 123:521–535, 1966.

[24] M. J. Klowden. Blood, sex, and the mosquito. *Bioscience*, 45(5):326–331, 1995.

[25] Ch. Kuehn. *Multiple time scale dynamics*, volume 191 of *Applied Mathematical Sciences*. Springer, Cham, 2015.

[26] J. Li. Malaria model with stage-structured mosquitoes. *Math. Biosci. Eng.*, 8(3):753–768, 2011.

[27] J. Li. New revised simple models for interactive wild and sterile mosquito populations and their dynamics. *J. Biol. Dyn.*, 11:316–333, 2017.
[28] J. Li, L. Cai, and Y. Li. Stage-structured wild and sterile mosquito population models and their dynamics. *J. Biol. Dyn.*, 11:79–101, 2017.
[29] G. A. Ngwa. On the population dynamics of the malaria vector. *Bulletin of mathematical biology*, 68(8):2161–2189, 2006.
[30] G. A. Ngwa, M. I. Teboh-Ewungkem, Y. Dumont, R. Ouifki, and J. Banasiak. On a three-stage structured model for the dynamics of malaria transmission with human treatment, adult vector demographics and one aquatic stage. *Journal of Theoretical Biology*, 481:202–222, 2019.
[31] G.A. Ngwa, B. M. Ghakanyuy, M. I. Teboh-Ewungkem, and J. Banasiak. Mating versus alternative blood sources as determinants to mosquito abundance and population resilience. *arXiv preprint arXiv:2412.05924*, 2024.
[32] P. Rashkov and B. W. Kooi. Complexity of host-vector dynamics in a two-strain dengue model. *J. Biol. Dyn.*, 15(1):35–72, 2021.
[33] P. Rashkov, E. Venturino, M. Aguiar, N. Stollenwerk, and B. W. Kooi. On the role of vector modeling in a minimalistic epidemic model. *Math. Biosci. Eng.*, 16(5):4314–4338, 2019.
[34] F. Rocha, M. Aguiar, M. Souza, and N. Stollenwerk. Time-scale separation and centre manifold analysis describing vector-borne disease dynamics. *International Journal of Computer Mathematics*, 90(10):2105–2125, 2013.
[35] O. Romoli, J. Serrato-Salas, C. Gapp, Y. Epelboin, P. F. Ivern, F. Barras, and M. Gendrin. Nutritional sex-specificity on bacterial metabolites during mosquito (aedes aegypti) development leads to adult sex-ratio distortion. *Biology Communications*, 7(1):123–135, 2024.
[36] G. Sallet. Mathematical epidemiology, 2018. https://hal.science/hal-04688889.
[37] H. L. Smith. *Monotone dynamical systems*, volume 41 of *Mathematical Surveys and Monographs*. American Mathematical Society, Providence, RI, 1995.
[38] H. L. Smith and P. Waltman. *The theory of the chemostat: dynamics of microbial competition*, volume 13. Cambridge University Press, 1995.
[39] K. Snyder, B. Kohler, and L. F. Gordillo. Mass action in two-sex population models: encounters, mating encounters and the associated numerical correction. *Letters in Biomathematics*, 4(1):101–111, 2017.
[40] M. Strugarek, H. Bossin, and Y. Dumont. On the use of the sterile insect release technique to reduce or eliminate mosquito populations. *Applied Mathematical Modelling*, 68:443–470, 2019.
[41] L. M. Styer, J. R. Carey, J.-L. Wang, and T. W. Scott. Mosquitoes do senesce: departure from the paradigm of constant mortality. *The American journal of tropical medicine and hygiene*, 76(1):111, 2007.
[42] H. R. Thieme. *Mathematics in population biology*. Princeton Series in Theoretical and Computational Biology. Princeton University Press, Princeton, NJ, 2003.
[43] A.N. Tikhonov, A.B. Vasileva, and A.G. Sveshnikov. *Differential equations*. Springer, Berlin, 1985.
[44] Vector Disease Control International. Mosquito biology 101: Life cycle. https://www.vdci.net/mosquito-biology-101-life-cycle/, 2024. Accessed: May 13, 2025.
[45] C Villarreal, G Fuentes-Maldonado, MH Rodriguez, and B Yuval. Low rates of multiple fertilization in parous anopheles albimanus. *Journal of the American Mosquito Control Association*, 10(1):67–69, 1994.
[46] E. O. Voit, H. A. Martens, and S. W. Omholt. 150 years of the mass action law. *PLoS Computational Biology*, 11(1):e1004012, 2015.
[47] S. Xue, M. Li, J. Ma, and J. Li. Sex-structured wild and sterile mosquito population models with different release strategies. *Math. Biosci. Eng.*, 16(3):1313–1333, 2019.

Received xxxx 20xx; revised xxxx 20xx; early access xxxx 20xx.